Saturated and unsaturated stokes-darcy fluid flow simulations within 3d interlock fabrics with capillary effects

Morgan Cataldi, Yanneck Wielhorski, Nicolas Moulin, Augustin Parret-Fréaud, Monica Francesca Pucci, Pierre-Jacques Liotier

SATURATED AND UNSATURATED STOKES-DARCY FLUID FLOW SIMULATIONS WITHIN 3D INTERLOCK FABRICS WITH CAPILLARY EFFECTS

M. Cataldi[1,2], Y. Wielhorski[2], N. Moulin[1], A. Parret-Freaud[3], M. F. Pucci[4] and P-J. Liotier[5]

[1] Mines Saint-Etienne, Univ Lyon, CNRS, UMR 5307 LGF, Saint-Etienne France
[2] Safran Aircraft Engines, Moissy-Cramayel, France
[3] Safran Tech, Magny-les-Hameaux, France
[4] LMGC, IMT Mines Ales, Univ Montpellier, CNRS, Ales, France
[5] Polymers Composites and Hybrids (PCH), IMT Mines Ales, Ales, France

Keywords: 3D interlock fabric, Flow simulations, Permeability, Stokes-Darcy coupling

ABSTRACT

Resin Transfer Moulding (RTM) is a process used in some composite parts manufacturing. A fibrous 3D interlock preform is firstly compacted to achieve the desired Fibre Volume Fraction (FVF), and is then impregnated with a polymer resin. Its flow within and between the homogeneous equivalent porous yarns has to be precisely understood to predict impregnation defects. The process setting is therefore monitored accordingly to the 3D interlock fabric permeability, defined from Darcy's law. A double-scale description is used to represent the fabric unit cells, taking into account both the mesoscopic yarn morphology and the intra-yarn FVF field. This field is then converted into a permeability tensor field that characterises the homogeneous equivalent intra-yarn properties. The unit cell has a multi-scale nature that leads consequently to multi-scale effects on the fluid flow. Darcy's equation is used as a model of the intra-tow flow and Stokes' equation is used between yarns. Therefore double-scale concerns on the effective fabric unit cell permeability tensor and the potentially resulting dry spot map. However, an accurate description of the resin flow within the homogeneous equivalent porous yarns is required to achieve this. A locally oriented intra-yarn permeability tensor field varying along yarns and a capillary stress tensor within them at the resin-air interface are added to model stationary and transient double-scale flow in 3D interlock fabrics.

1 INTRODUCTION

Thermoset resins are used in Resin Transfer Moulding (RTM) processes to fill 3D interlock fabrics in order to create high performance composite materials for aeronautics. Their mechanical properties are ensured through an accurate understanding of the process monitoring, and thus some key parameters. One of them is the fabric permeability, defined by Darcy's law, and thus must be precisely characterised through both flow experiments and numerical simulations. Since the fluid flows both within and around the porous yarns, this double-scale nature has to be taken into account within models. In addition, dry spots may appear at the end of the impregnation and hinder the mechanical properties of the composite parts manufactured. They are the result of both the process parameters and material properties of the fabric and porous yarns within it.

Our numerical simulations are performed on 3D woven models that are generated using techniques found in literature [1]. Many studies, both on idealized woven patterns [2] or X-ray micro-tomographies [3], analyse the variations of the fabric effective permeability. To estimate these variations, the intra-yarn permeability tensor is generally set to change homogeneously over the yarns between different simulations as in Geoffre et al. [4]. However, due to local deformations of the yarns during the fabric forming process, the intra-yarn FVF varies along the yarns. The 3D woven model generation used in this work takes into account this phenomenon to compute an intra-yarn FVF field, which is then used to get an intra-yarn permeability field.

Several methods exist to model the dual-scale flow problem both around and within the homogeneous equivalent porous yarns. Brinkman equation is a self-consistent way to proceed because the viscous dissipation term on both domains ensures the velocity and stress continuity at yarns outer interface [5]. However, this model can be inappropriate for domains with high properties contrast, such as in 3D interlocks. The Stokes-Darcy coupled problem is used in our simulations to model the double-scale fluid flow. It is solved by a mixed velocity – pressure Finite Element (FE) formulation with a monolithic approach detailed in previous works [6], and stabilised by a Variational Multiscale Method (VMS) known as the Algebraic SubGrid Scale (ASGS) method.

The fluid front in transient simulations is modelled by levelset [7] method, allowing to sharply describe the interface and is well suited for modelling its complex topologic changes, especially splitting and merging of interfaces. This is the case for capillary effects acting at the microscopic scale between the yarn fibres, and upscaled into a capillary force normal to the interface within the homogeneous equivalent porous yarns. A capillary stress tensor is used in our simulations and its components scalar value can come from experiments derived from soils sciences [8], a Washburn-Darcy equivalence [9], or numerical simulations at the microscopic scale [10].

2 DIGITAL MATERIALS

The software Multifil [11] is used to simulate the 3D interlock woven fabric unit cell by computing the yarn deformations with contact-friction interactions and an enriched kinematics beam model. Its inputs are the number of carbon fibres per yarn, their mechanical properties and their twist, along with the woven pattern. The resulting non-periodic unit cell is described by the meso-scale yarn morphology and the intra-yarn FVF. This last characteristic shown in Figure 1 is an upscaling of the microscopic intra-yarn morphology. Yarns are considered as homogeneous equivalent media characterised geometrically by consecutive sections attached to a neutral fibre, and by a permeability tensor for their porous nature. Both “as-woven” (not yet compacted) and “compacted” *(*as-manufactured) unit cells, along with their intra-yarn fibre volume fraction field are shown in Figure 1.

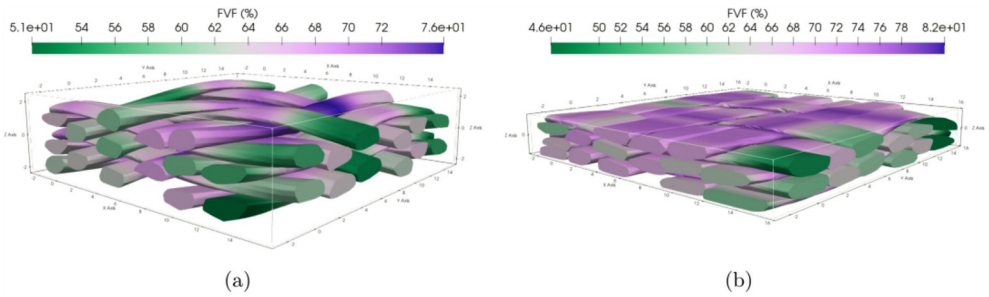

Figure 1: (a) as-woven and (b) compacted 3D interlock unit cells with their intra-yarn FVF field, respectively 29% and 58% global FVF.

3 METHODS

3.1 Intra-yarn permeability calculation

The intra-yarn permeability tensor is assumed to be as transversely isotropic in its principal coordinate system ($\mathbf{e_I}$,$\mathbf{e_{II}}$,$\mathbf{e_{III}}$) shown in Figure 2. According to Gebart’s law in hexagonal arrangement [12], the eigenvalues can be computed using Equations (1-2), where R = 2.6 µm is the fibre radius, V_f is the intra-yarn FVF value, K_L is the longitudinal permeability and K_T is the transverse one.

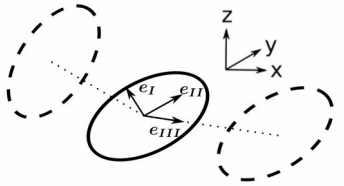

Figure 2: Local yarn section coordinate system.

$$K_L = \frac{8R^2}{53}\frac{(1-V_f)^3}{V_f^2}, \tag{1}$$

$$K_T = \frac{16R^2}{9\pi\sqrt{6}}\left(\sqrt{\frac{\pi}{2\sqrt{3}V_f}}-1\right)^{\frac{5}{2}}. \tag{2}$$

The resulting intra-yarn permeability values with their Probability Density Functions (PDF), means μ and standard deviations σ for both as-woven and compacted unit cells are shown in Figure 3.

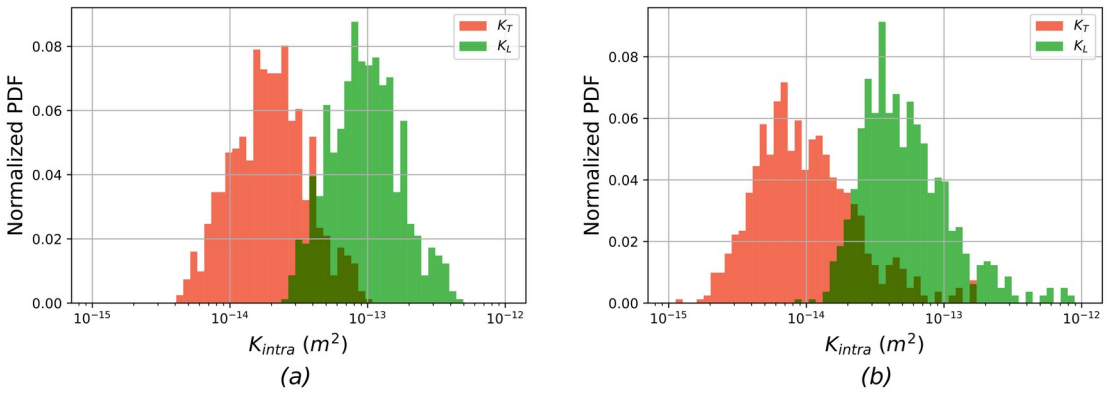

Figure 3: (a) as-woven (K_T ranges from 4.10^{-15} to 1.10^{-13} m² and K_L from 2.10^{-14} to 5.10^{-13} m²) and (b) compacted (K_T ranges from 1.10^{-15} to 2.10^{-13} m² and K_L from 8.10^{-15} to 9.10^{-13} m²) unit cells intra-yarn permeability Probability Density Functions (PDF).

3.2 Saturated flow

This part of study aims to perform simulations of the saturated double-scale fluid flow within both as-woven and compacted unit cells in order to compute their effective permeability tensor, commonly referred to as the saturated permeability. The steady-state flow is assumed to be laminar and incompressible. The fluid behavior is considered to be newtonian with a dynamic viscosity μ = 0.2 Pa.s. The physical model summarized in Figure 4 couples Stokes' equation in the domain around the yarns and Darcy's equation within them, where $\mathbf{K_{intra}}$ is the intra-yarn permeability tensor.

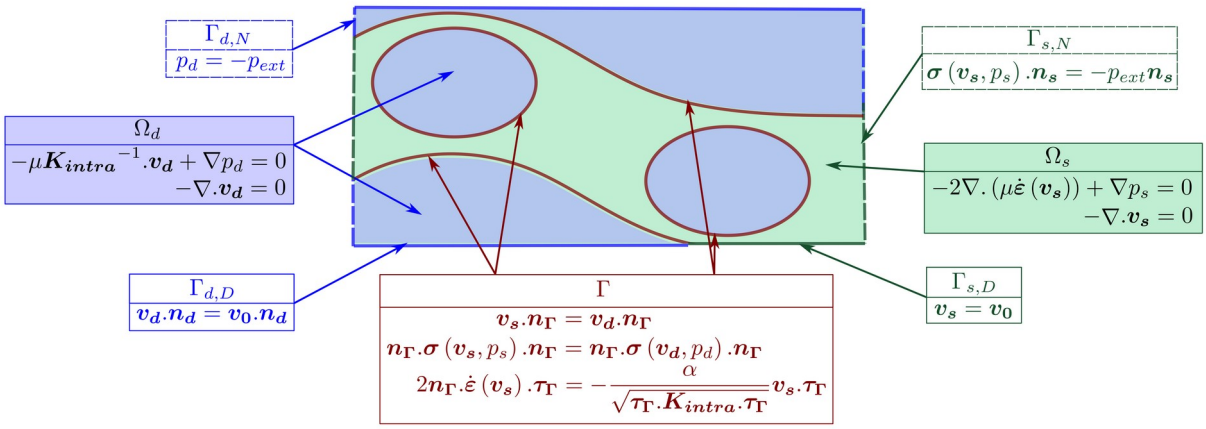

Figure 4: Physical model of the Stokes-Darcy coupled problem.

The unit cells are first meshed with voxels by Revoxel software, and then remeshed in an unstructured tetrahedral mesh by Mirax software [13]. The characteristic voxel size ranges from 70 to 100 µm, and the resulting tetrahedral meshes have between 1 and 8 million nodes. The complex yarn morphology is efficiently meshed with conformal interfaces between inter-yarn and intra-yarn domains. Figure 5 shows the resulting tetrahedral mesh, which is required for the P1/P1 formulation. The Stokes-Darcy coupled problem is solved by the Z-set software through a monolithic approach and a mixed velocity-pressure FE formulation. Since the P1/P1 formulation is not stable, a Variational Multi-Scale (VMS) method is introduced, specifically the Algebraic SubGrid Scale (ASGS) method to add stabilizing terms to the initial formulation. The weak formulation of the stabilized Stokes-Darcy coupled problem can be found in [6].

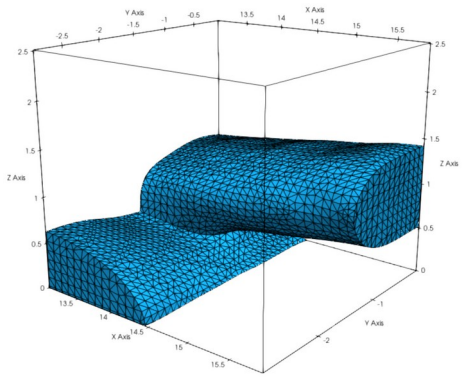

Figure 5: Tetrahedral mesh of the yarns (corner of the as-woven unit cell described in Figure 1).

Velocity and pressure fields are retrieved from the saturated flow simulations corresponding to a main flow in the X, Y and Z directions. The unit cell effective permeability tensor $\mathbf{K}_{\mathbf{eff}}$ is then calculated by using the 3D-generalized Darcy's law:

$$v = \frac{-1}{\mu} K_{eff} . \nabla p \, . \tag{3}$$

All its nine components are computed because no assumptions are made on it. The permeability tensor $\mathbf{K}_{\mathbf{eff}}$ is diagonalized afterwards to retrieve its eigenvectors and eigenvalues.

3.3 Transient flow

The aim here is to perform simulations of the transient double-scale fluid flow within both as-woven and compacted unit cells, where resin progressively replaces air within the preform during the filling process. In addition to the Stokes-Darcy coupling and the numerical strategy to solve it, previously described, the resin-air interface needs to be modelled and tracked through time. A levelset field φ is thus used to describe this interface by the isosurface defined by: φ = 0. This field is convected accordingly to the transport equation and the fluid velocity $\boldsymbol{v}$:

$$\frac{\partial \varphi}{\partial t} + v \,.\, \nabla \varphi = 0 \,. \tag{4}$$

A time-implicit discretization is achieved with a Crank-Nicolson scheme and a Streamline Upwind Petrov-Galerkin (SUPG) stabilizes the FE formulation. Since the field φ is a signed distance to the interface φ = 0, this property needs to be ensured through the simulation.

Moreover, different viscosity values between resin and air are used for bi-phasic flow simulations: $\mu_{resin} = 0.2$ Pa.s and $\mu_{air} = 1.10^{-3}$ Pa.s. Capillary effects occurring at the microscopic scale between the yarn fibres are to be upscaled at the mesoscopic scale within the homogeneous equivalent porous yarns. A transverse isotropic capillary stress tensor $\boldsymbol{\sigma_{cap}}$ is thus introduced within the Darcy domain to account for the pressure discontinuity at the resin-air interface of normal $\boldsymbol{n}$ such as:

$$n \,.\, \sigma_{cap} \,.\, n = [\, p \,]_{\Gamma_{l/a}} \,. \tag{5}$$

These two new features lead to a discontinuity of both pressure and gradient pressure within the mesh elements crossed by the interface as shown in Figure 6. This point is firstly addressed by splitting these elements into sub-elements containing new integration points with the Surface Local Reconstruction (SLR) method. And it is secondly addressed by enriching the pressure field with new degrees of freedom which are then condensed with the original ones. Finally, a weak coupling between the Stokes-Darcy and levelset finite element problems allows to numerically solve the transient double-scale fluid flow within the unit cells. All details about the simulation of a transient flow and the introduction of the capillary stress tensor in the Darcy FE problem can be found in [14].

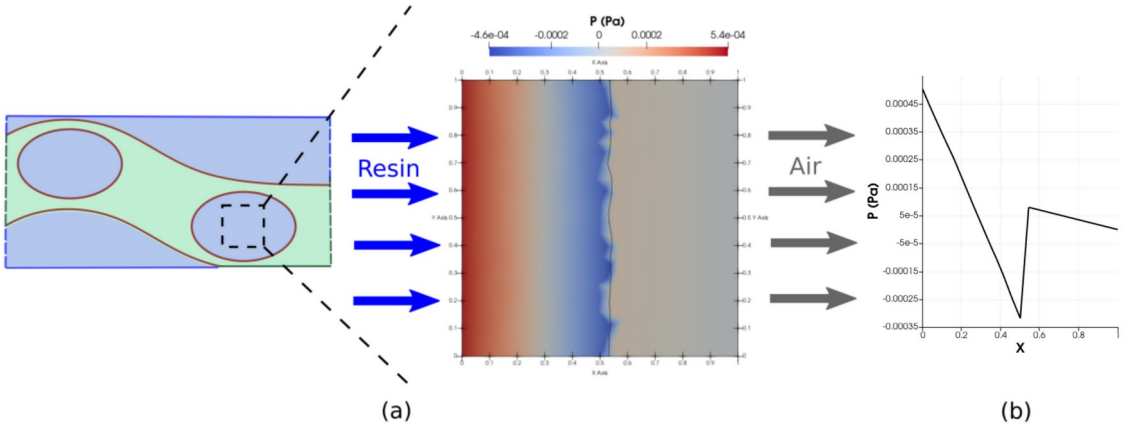

Figure 6: Pressure field within a Darcy unit square during a transient flow with a capillary pressure $P_{cap} = 5.10^{-4}$ Pa, the pressure profile is plotted along the line Y=0,5.

4 RESULTS AND PERSPECTIVES

Analysis of the streamlines in the simulations of the double-scale saturated flow in Figure 7 suggests that the majority of the fluid flows around the yarns, which is highlighted by the greater velocity magnitude in these areas. The low intra-yarn permeability values, in the range of 10^{-12} to 10^{-14} m^2

compared to the inter-yarn channels width explains why the fluid does not flow well through the yarns. As a result, variations of the effective permeability tensor $\mathbf{K}_{\mathbf{eff}}$ are induced by variations of the intra-yarn FVF field in a very limited way.

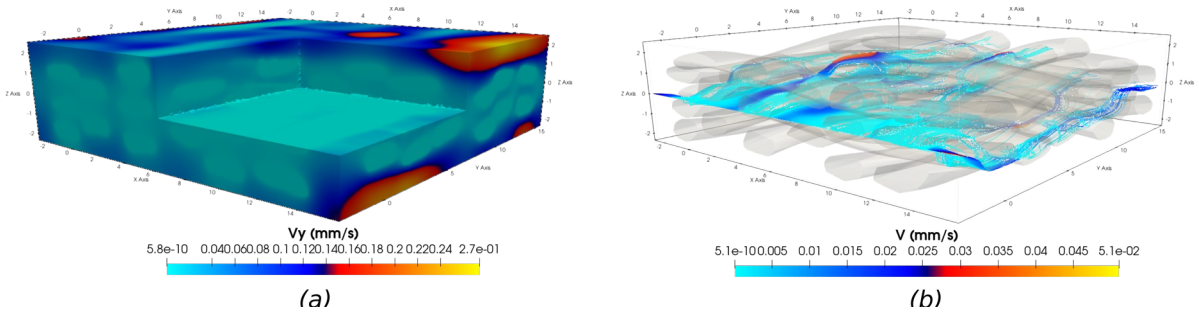

Figure 7: (a) Velocity field and (b) streamlines from the inlet boundary in the as-woven unit cell.

On the contrary, changes in the mesoscopic unit cell morphology are of first importance when studying its permeability tensor $\mathbf{K}_{\mathbf{eff}}$. This is highlighted in Table 1, where the fabric compaction leads to a reduction of about 2 orders of magnitudes for its diagonal components K_{xx}, K_{yy} and K_{zz}. This is due to the huge reduction of inter-yarn spaces trough the compaction, thus increasing the unit cell global FVF value (with porous yarns) from 29% to 58%.

FVF (%)	Kxx (m²)	Kyy (m²)	Kzz (m²)
29	6.10^{-8}	9.10^{-8}	2.10^{-8}
58	5.10^{-10}	2.10^{-9}	2.10^{-9}

Table 1: Permeabilities of the as-woven (29% FVF) and compacted (58% FVF) unit cells.

Moreover, the velocity field shown in Figure 7 highlights preferential edge flows characterized by high velocity magnitudes. This implies that, in addition to flowing around the yarns, the fluid mainly flows near the unit cell boundaries. Consequently, the effective permeability tensor $\mathbf{K}_{\mathbf{eff}}$ of the unit cell is overestimated. To take it into account, a geometrical reduction of its boundaries is performed, as illustrated in Figure 8, prior to the numerical simulation in order to ensure that the fluid flows within the weaving pattern. This reduction of 10% eliminates most of the preferential edge flows and thus allows for a more accurate computation of the permeability tensor, as shown in Table 2.

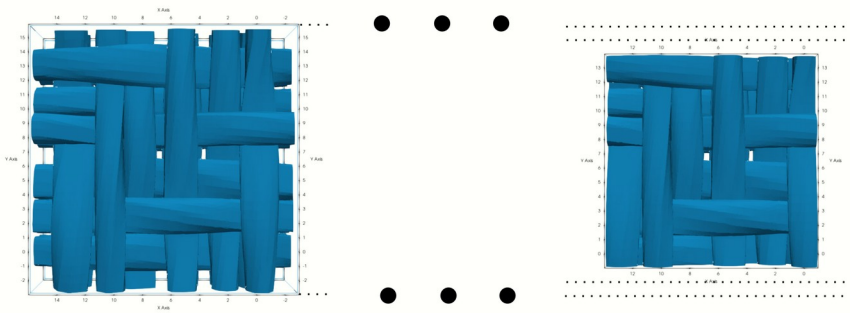

Figure 8: Top view of the unit cell reduction from 0% (left) to 20% (right).

Unit Cell Reduction (%)	Kxx (m²)	Kyy (m²)	Kzz (m²)
0	6.10^{-8}	9.10^{-8}	2.10^{-8}
10	4.10^{-8}	6.10^{-8}	3.10^{-9}
20	4.10^{-8}	5.10^{-8}	2.10^{-9}

Table 2: Permeabilities of the whole and reduced as-woven unit cell.

A numerical simulation of the transient flow in the Z direction was performed on the as-woven unit cell. The as-woven unit cell filling can be seen in Figure 10 at three different stages. Further works will focus on the pressure field enrichments to better account for the previously mentioned discontinuities, along with the implementation of the capillary stress tensor obtained from experiments [9] at the resin-air interface within the yarns. This will finally result in a complete transient double-scale flow simulation within 3D interlock unit cells with a well designed model of the flow advance both around and within the yarns.

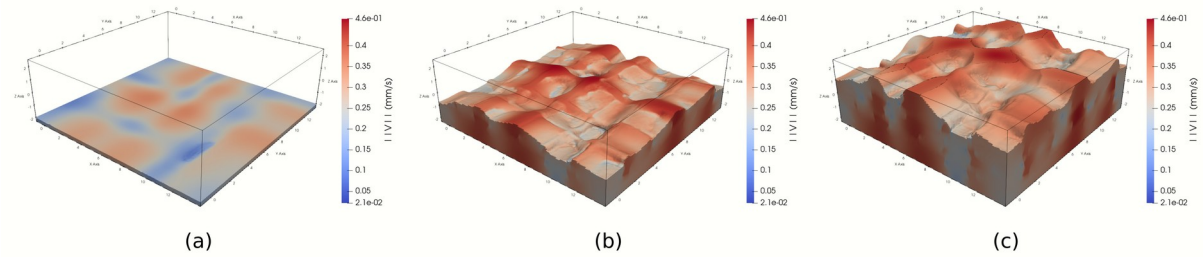

Figure 10: Filling simulation of the as-woven unit cell from the bottom: (a) first, (b) middle and (c) last time steps.

ACKNOWLEDGEMENTS

Authors acknowledge the support of a PhD grant N°2021/0156 from ANRT and Safran Aircraft Engines.

REFERENCES

[1] Y. Wielhorski, *et al.*, Numerical modeling of 3d woven composite reinforcements: A review, *Composites Part A: Applied Science and Manufacturing* 154 (2022) 106729.

[2] Q. Wang, *et al.,* A note on permeability simulation of multifilament woven fabrics. *Chemical Engineering Science*. 2006 dec; 61 (24).

[3] MA. Ali, *et al.,* XCT-scan assisted flow path analysis and permeability prediction of a 3D woven fabric. *Composites Part B: Engineering*. 2019 nov; 176.

[4] A. Geoffre, *et al.,* Influence of intra-yarn flows on whole 3D woven fabric numerical permeability: from Stokes to Stokes-Darcy simulations. *International Journal of Multiphase Flow*. 2020 aug; 129.

[5] D. Shou, *et al.,* Transverse permeability determination of dual-scale fibrous materials. *International Journal of Heat and Mass Transfer*. 2013 mar; 58 (1-2).

[6] L. Abouorm, *et al.*, Stokes–darcy coupling in severe regimes using multiscale stabilisation for mixed finite elements: monolithic approach versus decoupled approach, *European Journal of Computational Mechanics* 23 (2014) 113–137.

[7] S. Osher, *et al.*, Level set methods: an overview and some recent results, *Journal of computational physics*, Vol. 169 No. 2, pp 463-502, 2001.

[8] H. Teixidó, *et al.*, Measurement and modelling of dynamic fluid saturation in carbon reinforcements, *Composites Part A: Applied Science and Manufacturing*, 169 (2023) 107520.

[9] M.F. Pucci, *et al.*, Capillary wicking in a fibrous reinforcement – Orthotropic issues to determine the capillary pressure components, *Composites Part A: Applied Science and Manufacturing*, 77 (2015) 133-141.

[10] A. Geoffre, *et al.*, Reappraisal of Upscaling Descriptors for Transient Two-Phase Flows in Fibrous Media. *Transp Porous Med* 147, 345–374 (2023).

[11] D. Durville, *et al*. "Determining the initial configuration and characterizing the mechanical propreties of 3D angle-interlock fabrics using finite element simulation". *International Journal of Solids and Structures*, Vol. 154, pp 97-103, 2018.

[12] B.R. Gebart, "Permeability of unidirectional reinforcements for RTM". *Journal of Composite Materials*, Vol. 26, No. 8, pp 1100-1133, 1992.

[13] A. Rassineux, Robust conformal adaptive meshing of complex textile composites unit cells, *Composite Structures* 279 (2022) 114740.

[14] K. Andriamananjara, *et al*. "Numerical modeling of local capillary effects in porous media as a pressure discontinuity acting on the interface of a transient bi-fluid flow". *International Journal of Material Forming*, Vol. 12, No. 4, pp 675-691, 2018.